International Journal of Research
Available at https://edupediapublications.org/journals
e-ISSN: 2348-6848
p-ISSN: 2348-795X
Volume 04 Issue 14
November 2017

Control of Grid Connected Photovoltaic System Using Both Fuzzy and Ann Controller for Constant Power Generation

[1]P. SUJATHA, [2]A.VIJAY KUMAR
[1]PG Scholar, B. V Raju Institute Of Technology (Autonomous) College, Narsapur, Hyderabad, Telangana, India.
[2]Assistant Professor, B. V Raju Institute Of Technology (Autonomous) College, Narsapur, Hyderabad, Telangana, India.

***ABSTRACT*: In this project we are implementing an improved control strategy such as the incremental method of the maximum power which is feed to the PV systems with ANFIS controller which is combination of fuzzy and ann controller which is proposed to make sure about the smooth and fast transition between Constant Power Generation (CPG) and maximum power point tracking ,and also by the proposed control strategy we can always achieved the stable operation, Regardless of the solar irradiance levels and high-performance. Which can be regulate by the PV output power according to any set-point, and it also force the PV systems to operate at the left side of the maximum power point without any stability problems. Here we are using the ANFIS controller comparing the other controller because of the better performance . Neuro-fuzzy is a combination of ANN and fuzzy logic. By comparing all these techniques, the neuro-fuzzy controller is the lot of advantages; i.e the normalized error obtained from neuro fuzzy logic was lower. By using the ANFIS controller we get the better performance and also for the reduction of uncertain effects in the system control and improves the efficiency. Simulation results have been verified in the effectiveness manner by using the proposed CPG control in terms of high accuracy, stable transitions, and fast dynamics.**

Index Terms - Active power control, constant power control, maximum power point tracking, PV systems, power converters, ANN control and fuzzy control.

INTRODUCTION

In the recent year, Maximum Power Point Tracking (MPPT) operation is necessary in the grid-connected PV systems in order to get the maximize power from the energy yield. PV installations is need for the advance power control schemes and along with the regulations to decrease impacts from PV systems such as the overloading the power grid. For the German Federal Law: Renewable Energy Sources Act in which the PV systems with the rated power below 30 kWp which have the limit for the maximum which is feed to the power (e.g. 70 % of the rated power) which can be remotely controlled by the utility like the active power control which is refered as the Constant Power Generation (CPG) control or an absolute power control which is described in the Danish grid code in which CPG concept which have been presented which is reveals by the most cost-effective way to achieve the CPG control is by modifying the MPPT algorithm at the PV inverter level. Specifically, the PV system is operated in the MPPT mode, when the PV output power Ppv is below the setting-point Plimit.

$$P_{PV} = \begin{cases} P_{MPPT}, & \text{when } P_{PV} \le P_{limit} \\ P_{limit}, & \text{when } P_{PV} > P_{limit} \end{cases} \quad (1)$$

Moreover, whenever the output power reach the Limit, then the output power of the PV system will be kept constant, i.e., Ppv = Plimit, which leading to the constant active power which is injected as shown in (1) and it also illustrated in Fig. 1 In terms of the algorithms and the CPG which is based upon the Perturb and Observe (P&O-CPG) algorithm which was introduced by the single stage PV systems . Moreover during the operating area of the CPG control which is limited at the right side of the Maximum Power Point (MPP) of the PV arrays (CPP-R), due to its single-stage configuration. Unfortunately it will reduce the robustness of the control algorithm when the PV systems is experience with the fast decrease during the irradiance time.

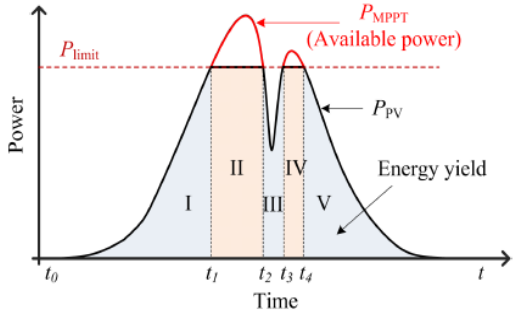

Fig. 1. Constant Power Generation (CPG) concept: 1) MPPT mode during I, III, V, and 2) CPG mode during II, IV [6].

The operating point may go through the open-circuit condition which is illustrated and shown in the Fig. 2. A two-stage grid-connected PV is implemented to extend the operating area of the P&O-CPG algorithm. And also by regulating the PV output power which at the left side of the MPP (CPP-L) as shown in Fig. 2, where the stable CPG

International Journal of Research
Available at https://edupediapublications.org/journals
e-ISSN: 2348-6848
p-ISSN: 2348-795X
Volume 04 Issue 14
November 2017

operation is always achieved by the operating point which will never "fall off the hill" during a fast reduce in the irradiance.

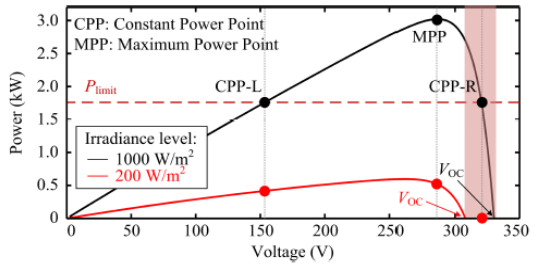

Fig. 2. Stability issues of the conventional CPG algorithms, when the operating point is normally located at the right side of the MPP.

Both the P&O-CPG algorithm can be applied to any two-stage single-phase PV system.

CONVENTIONAL CPG ALGORITHM

System Configuration

As shown in the Fig. 3 shows the basic hardware configuration of the two-stage single-phase grid-connected PV system and its control structure. The CPG control is developed in the boost converter, which have been explained in the next section.

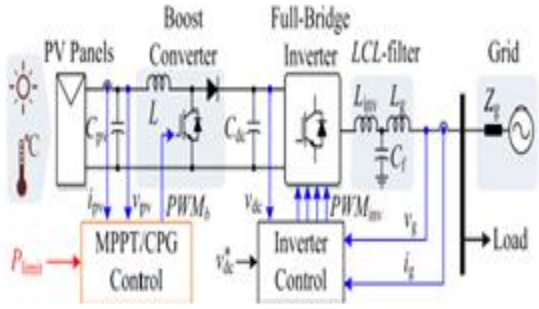

Fig. 3. Simulation of schematic and overall control structure of a two-stage singlephase grid-connected PV system

The full-bridge inverter control is realized by the cascaded control ,here the DC-link voltage is kept constant throughout the control of the AC grid current, which is an inner loop . an active power is injected to the grid, which meaning that the PV system operates at a unity power factor. Not only that have been mentioned above and the two-stage configuration can extend the operating range of both the MPPT and CPG algorithms. In the two-stage case, the PV output voltage vpv can be lower (e.g., at the left side of the MPP), and then it can be stepped up by the boost converter to match the required DC-link voltage (e.g., 450 V) [10]. This is not the case for the single-stage configuration, where the PV output voltage vpv is directly fed to the PV inverter and has to be higher than the grid voltage level (e.g., 325 V)to ensure the power delivery .

Operational Principle

The operational principle of the conventional P&O-CPG algorithm is illustrated in Fig. 4. It can be divided into two modes: a) MPPT mode (Ppv Plimit), where the P&O algorithm should track the maximum power; b) CPG mode (Ppv > Plimit), where the PV output power is limited at Plimit. During the MPPT operation, the behavior of the algorithm is similar to the conventional P&O MPPT algorithm - the operating point will track and oscillate around the MPP [13].

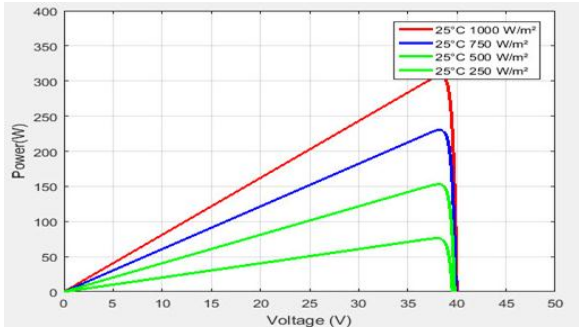

Fig. 4. Operational principle of the Perturb and Observe based CPG algorithm (P&O-CPG), where the operating point is regulated to the left side of the MPP considering stability issues.

In the case of the CPG operation, the PV voltage vpv is continuously perturbed toward a point referred to as Constant Power Point (CPP), i.e., Ppv = Plimit. After a number of iterations, the operating point will reach and oscillate around the CPP. Although the PV system with the P&O-CPG control can operate at both CPPs, only the operation at the left side of the MPP (CPP-L) is focused for the stability concern. The control structure of the algorithm is shown in Fig. 5, where v* pv can be expressed as

$$v^*_{PV} = \begin{cases} v_{MPPT}, & \text{when } P_{PV} \le P_{limit} \\ v_{pv,n-v_{step}}, & \text{when } P_{PV} > P_{limit} \end{cases} \quad (2)$$

where vMPPT is the reference voltage from the MPPT algorithm (i.e., the P&O MPPT algorithm), vpv,n is the measured PV voltage, and vstep is the perturbation step size.

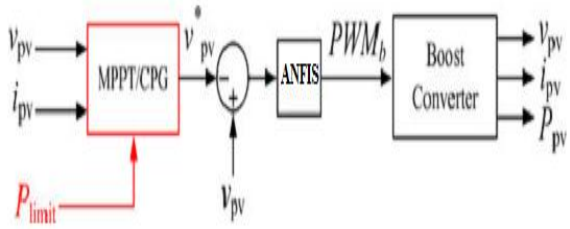

Fig. 5. Control structure of the Perturb and Observe based CPG algorithm (P&O-CPG) where a fuzzy control is adopted.

International Journal of Research
Available at https://edupediapublications.org/journals
e-ISSN: 2348-6848
p-ISSN: 2348-795X
Volume 04 Issue 14
November 2017

Issues Of The P&O-CPG Algorithm

The P&O-CPG algorithm has a satisfied performance under slow changing irradiance conditions, e.g., during a clear day, when the operating point is at the left side of the MPP, as shown in Fig. 6(a). However, irradiance fluctuation that may happen in a cloudy day will result in overshoots and power losses as shown in Fig. 6(b).

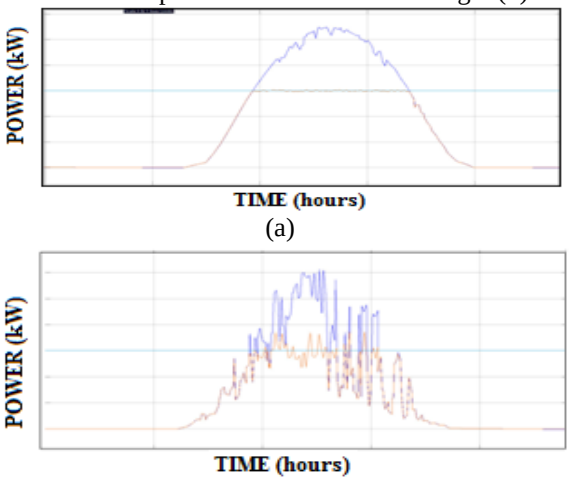

Fig. 6. simulation results of the Perturb and Observe based CPG algorithm (P&O-CPG) under two daily conditions: (a) clear day and (b) cloudy day.

This can be further explained using the operation trajectory of the PV system presented in Fig. Assuming that the PV system is operating in MPPT mode initially and the irradiance level suddenly increases, the PV power Ppv is basically lifted by the change in the irradiance, as it can be seen from the black arrow trajectory (i.e., A!B!C). As a consequence, large power overshoots may occur. Similarly, if the PV system is operating in the CPG operation (e.g., at CPP-L) and the irradiance suddenly drops, the output power Ppv will make a sudden decrease, as shown in Fig. (i.e., CID). It will take a number of iterations until the operating point reaches the new MPP (i.e., E) at that irradiance condition (i.e., 200 W/m2), and resulting in loss of power generation.

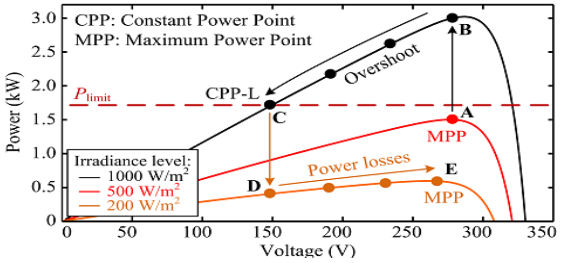

Fig. 7. Operating trajectory of the algorithm during a fast changing irradiance condition resulting in overshoot (black arrow) and power losses (orange arrow).

HIGH-PERFORMANCE P&O-CPG ALGORITHM

According to the above, two main tasks exist - minimizing the overshoots and minimizing the power losses during the fast changing irradiance condition which has to be addressed in the case of CPG operation. The proposed high-performance P&O-CPG algorithm can effectively solve those issues. A. Minimizing Overshoots Increasing the perturbation step size is a possibility to minimize the overshoots as the tracking speed is increased. Specifically, a large step size can reduce the required number of iterations to reach the corresponding CPP. Notably, the step size modification should be enabled only when the algorithm detects a fast increase in the Irradiance Condition (IC), which can be illustrated as

$$IC = \begin{cases} 1, & \text{when } P_{PV,n} - P_{limit} > \epsilon_{inc} \\ 0, & \text{when } P_{PV,n} - P_{limit} \le \epsilon_{inc} \end{cases} \quad (3)$$

with Ppv,n being the measured PV power at the present sampling, and "inc being the criterion, which should be larger than the steady-state power oscillation of the PV panels. When a fast increase in the IC is detected (i.e., IC = 1), an adaptive step size is then employed, where the step size is calculated based on the difference between Plimit and Ppv,n as it is given in (4). By doing so, the large step size will be used initially and the step size will continuously be reduced as the operating point approaches to the CPP.

$$v^*_{PV} = v_{pv,n} - \left[(P_{pv,n} - P_{limit}) \frac{P_{limit}}{P_{mp.\gamma}} \right] . v_{step} \quad (4)$$

where vpv is the reference output voltage of the PV arrays, vpv,n and Ppv,n are the measured output voltage and power of the PV array at the present sampling, respectively. Pmp is the rated power. Vstep is the original step size of the P&O-CPG algorithm. The term Plimit=Pmp is introduced to alleviate the step size dependency in the level of Plimit. is a constant which can be used to tune the speed of the algorithm.

Minimizing Power Losses

As explained in Fig. when the CPG operating point is at the left side of the MPP, the P&O-CPG algorithm requires a number of iterations to reach the new MPP during a fast decease in irradiance, leading to power losses. In fact, the operating point of the PV system does not change much if the PV system is operating in the MPPT under different irradiance levels as shown in Fig. 8. Notably, the detection of the decreased IC as well as the Previous Operating Mode (POM) is also important for minimizing the power losses:

$$IC = \begin{cases} 1, & \text{when } P_{PV,n-1} - P_{pv,n} > \varepsilon_{dec} \\ 0, & \text{when } P_{PV,n-1} - P_{pv,n} \le \varepsilon_{dec} \end{cases} \quad (5)$$

International Journal of Research
Available at https://edupediapublications.org/journals
e-ISSN: 2348-6848
p-ISSN: 2348-795X
Volume 04 Issue 14
November 2017

$$POM = \begin{cases} CPG, & when \left| P_{limit} - P_{PV,n-1} \right| > \varepsilon_{ss} \\ MPPT, & when \left| P_{limit} - P_{PV,n-1} \right| \leq \varepsilon_{ss} \end{cases} \quad (6)$$

where "dec and "ss are criteria to determine the fast irradiance decrease and the CPG operating mode, respectively. Ppv,n-1 is the measured PV power at the previous sampling. For example, the value of "ss can be chosen as 1-2 % of the rated power of the PV system, which is normally higher than the steady-state error in the PV power of the P&O-CPG algorithm. When a fast decrease (i.e., IC = 1) is detected during the CPG to MPPT transition according to (6), a constant voltage given by (7) is applied to the PV system in order to accelerate the tracking speed (i.e., minimize the power losses). The constant voltage can be approximated as 71-78 % of the open circuit voltage VOC, as illustrated in Fig. 7.

$$v_{pv}^{*} = k.V_{OC}, where\ 0.71 \leq k < 0.78 \quad (7)$$

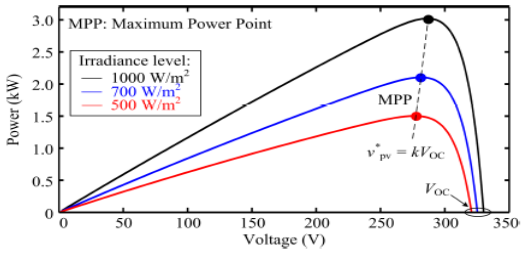

Fig. 7. Power-voltage (P-V) curves of the PV arrays, where the voltage at the MPP is almost constant especially at a higher irradiance level .

By doing so, the operating point can be instantaneously moved close to the MPP in one perturbation, resulting in a significant reduction in the number of iterations until the operating point reaches the MPP.

NEURO FUZZY

In the field of artificial intelligence, neuro-fuzzy refers to combinations of artificial neural networks and fuzzy logic. Neuro-fuzzy was proposed by J. S. R. Jang. Neuro-fuzzy hybridization results in a hybrid intelligent system that synergizes these two techniques by combining the human-like reasoning style of fuzzy systems with the learning and connectionist structure of neural networks.

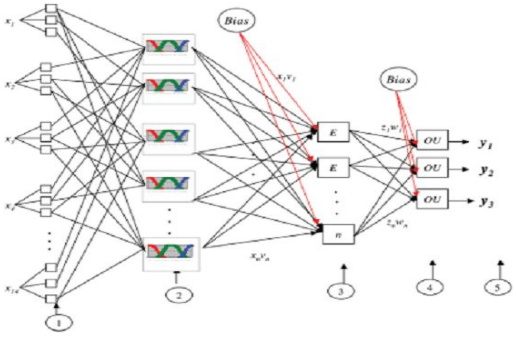

Fig. 8 A network of nodes using neuro-fuzzy integrated approach

Neuro fuzzy has many advantages i.e it can be stated that the normalized error obtained from neurofuzzy logic was lower. Compared to the multiple regression analysis neurofuzzy logic showed higher accuracy in prediction for the five outputs studied. Rule sets generated by neurofuzzy logic are completely in agreement with the findings based on statistical analysis and advantageously generate understandable and reusable knowledge. Neurofuzzy logic is easy and rapid to apply and outcomes provided knowledge not revealed via statistical analysis. the most important advantage of neural networks is their adaptivity. Neural networks can automatically adjust their weights to optimize their behavior as pattern recognizers, decision makers, system controllers, predictors, etc.

FUZZY LOGIC CONTROLLER

In FLC, basic control action is determined by a set of linguistic rules. These rules are determined by the system. Since the numerical variables are converted into linguistic variables, mathematical modeling of the system is not required in FC.

International Journal of Research
Available at https://edupediapublications.org/journals
e-ISSN: 2348-6848
p-ISSN: 2348-795X
Volume 04 Issue 14
November 2017

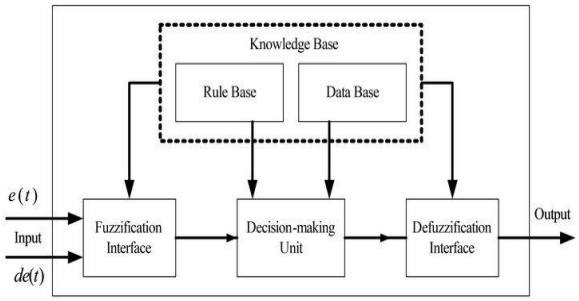

Fig.7.Fuzzy logic controller

The FLC comprises of three parts: fuzzification, interference engine and defuzzification. The FC is characterized as i. seven fuzzy sets for each input and output. ii. Triangular membership functions for simplicity. iii. Fuzzification using continuous universe of discourse. iv. Implication using Mamdani's, 'min' operator. v. Defuzzification using the height method.

TABLE I: Fuzzy Rules

Change in error	Error						
	NB	NM	NS	Z	PS	PM	PB
NB	PB	PB	PB	PM	PM	PS	Z
NM	PB	PB	PM	PM	PS	Z	Z
NS	PB	PM	PS	PS	Z	NM	NB
Z	PB	PM	PS	Z	NS	NM	NB
PS	PM	PS	Z	NS	NM	NB	NB
PM	PS	Z	NS	NM	NM	NB	NB
PB	Z	NS	NM	NM	NB	NB	NB

Fuzzification: Membership function values are assigned to the linguistic variables, using seven fuzzy subsets: NB (Negative Big), NM (Negative Medium), NS (Negative Small), ZE (Zero), PS (Positive Small), PM (Positive Medium), and PB (Positive Big). The Partition of fuzzy subsets and the shape of membership CE(k) E(k) function adapt the shape up to appropriate system. The value of input error and change in error are normalized by an input scaling factor. In this system the input scaling factor has been designed such that input values are between -1 and +1. The triangular shape of the membership function of this arrangement presumes that for any particular E(k) input there is only one dominant fuzzy subset. The input error for the FLC is given as

$$E(k) = \frac{P_{ph(k)} - P_{ph(k-1)}}{V_{ph(k)} - V_{ph(k-1)}} \quad (7)$$

$$CE(k) = E(k) - E(k\text{-}1) \quad (8)$$

Inference Method: Several composition methods such as Max–Min and Max-Dot have been proposed in the literature. In this paper Min method is used. The output membership function of each rule is given by the minimum operator and maximum operator. Table 1 shows rule base of the FLC.

Defuzzification: As a plant usually requires a non-fuzzy value of control, a defuzzification stage is needed. To compute the output of the FLC, „height" method is used and the FLC output modifies the control output. Further, the output of FLC controls the switch in the inverter. In UPQC, the active power, reactive power, terminal voltage of the line and capacitor voltage are required to be maintained. In order to control these parameters, they are sensed and compared with the reference values. To achieve this, the membership functions of FC are: error, change in error and output

The set of FC rules are derived from

$$u=-[\alpha E + (1-\alpha)*C] \quad (9)$$

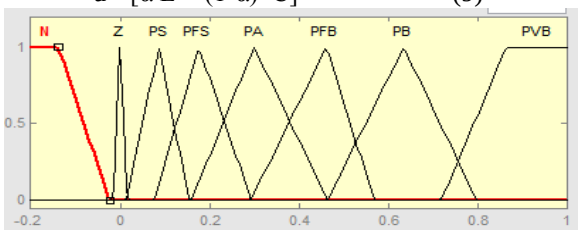

Fig 8 input error as membership functions

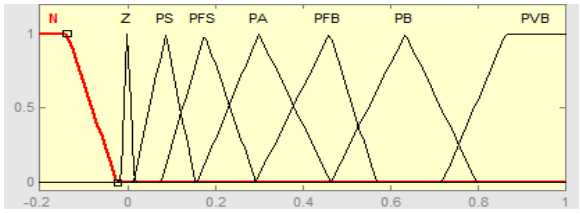

Fig 9 change as error membership functions

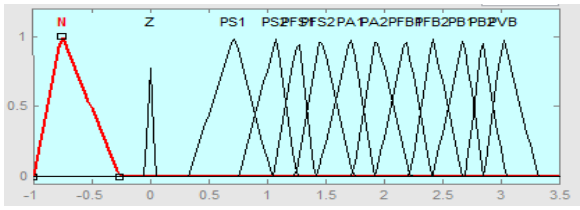

Fig.10 output variable Membership functions

Where α is self-adjustable factor which can regulate the whole operation. E is the error of the system, C is the change in error and u is the control variable.

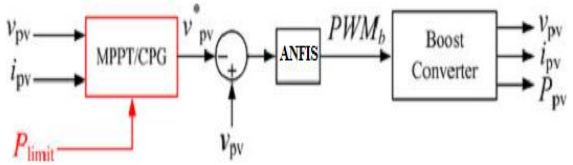

Fig 11. Control structure of the Perturb and Observe based CPG algorithm (P&O-CPG), where a Adaptive Neuro Fuzzy Interface System (ANFIS) is adopted.

ARTIFICIAL NEURAL NETWORK

Introduction

In the last few decades, as the chemists have get accustomed to the use of computers and consequently to the implementation of different complex statistical methods. With the increasing accuracy and precision of analytical measuring methods it become clear that all effects that are of interest cannot be described by simple uni-variate and

even not by the linear multivariate correlations precise, a set of methods, that have recently found very intensive use among chemists are the artificial neural networks (or ANNs for short).

Therefore, the analytical chemists are always eager to try all new methods that are available to solve such problems. One of the methods, or to say more Due to the fact that this is not one, but several different methods featuring a wide variety of different architectures learning strategies and applications.

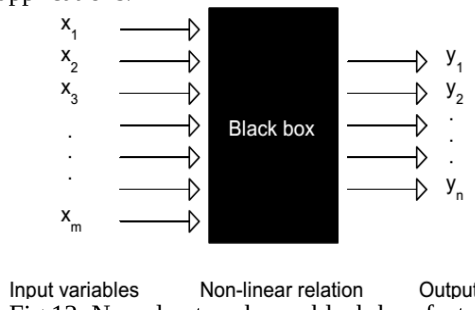

Fig 12. Neural network as a black-box featuring the non-linear relationship between the multivariate input variables and multi-variate responses

BASIC CONCEPTS OF ANNS

Artificial neuron is supposed to mimic the action of a biological neuron, i.e., to accept many different signals, xi, from many neighbouring neurons and to process them in a pre-defined simple way. Depending on the outcome of this processing, the neuron j decides either to fire an output signal yj or not. The output signal (if it is triggered) can be either 0 or 1, or can have any real value between 0 and 1 (Fig. 2) depending on whether we are dealing with 'binary' or with 'real valued' artificial neurons, respectively.

The first function is a linear combination of the input variables, x1 , x2, ... xi, ... xm, multiplied with the coefficients, wji, called 'weights', while the second function serves as a 'transfer function' because it 'transfers' the signal(s) through the neuron's axon to the other neurons' dendrites.

$$Net_j = \sum_{i=1}^{m} w_{ji} x_i \qquad (10)$$

$$y_j = out_j = 1 \Big/ \{1 + exp[-\alpha_j(Net_j + \theta_j)]\} \qquad (11)$$

The weights wji in the artificial neurons are the analogues to the real neural synapse strengths between the axons firing the signals.

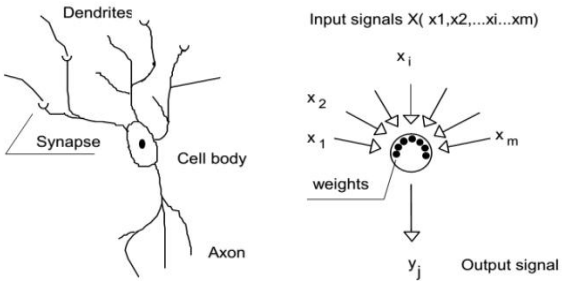

Figure 13. Comparison between the biological and artificial neuron. The circle mimicking the neuron's cell body represents simple mathematical procedure that makes one output signal yj from the set input signals represented by the multi-variate vector X.

It is important to understand that the form of the transfer function, once it is chosen, is used for all neurons in the network, regardless of where they are placed or how they are connected with other neurons.

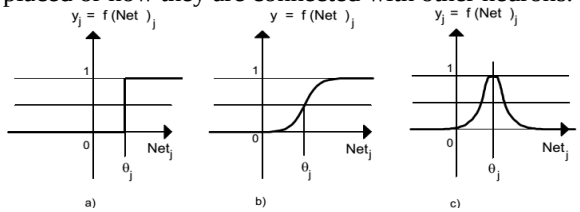

Figure 14. Three different transfer functions: a threshold (a), a sigmoidal (b) and a radial function (c). The parameter qj in all three functions decides the Netj value around which the neuron is most selective.

Therefore, Figure shows actually a 2-layer and a 3-layer networks with the input layer being inactive.

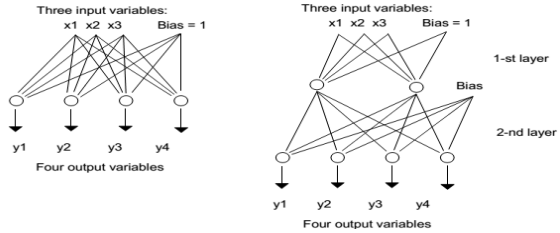

Figure 15. One-layer (left) and two-layer (right) ANNs. The ANNs shown can be applied to solve a 3-variable input 4-responses output problem

SIMULATION VERIFICATION

Solutions to improve the dynamic performance of the P&OCPG algorithm have been discussed above. Parameters of the proposed high-performance P&O-CPG algorithm are designed as: = 10, k = 0.715, "inc = 50 W, "dec = 100 W, and "ss = 30 W. Simulation are carried out referring to Fig.17, and the system parameters are given in Table II.

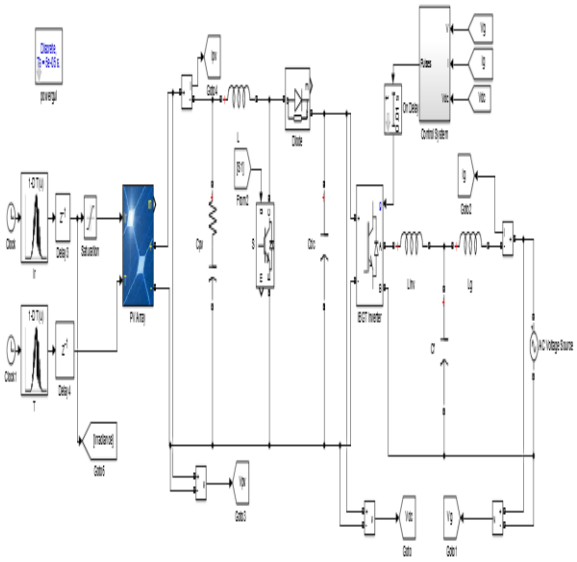

Fig.16.Block diagram of simulation

Table II
Parameters Of The Two-Stage Single-Phase Pv System

Boost converter inductor	L = 1.8 mH
PV-side capacitor	C_{pv} = 1000 μF
DC-link capacitor	C_{dc} = 1100 μF
LCL-filter	L_{inv} = 4.8 mH, L_g = 4 mH, C_f = 4.3 μF
Switching frequency	Boost converter: f_b = 16 kHz, Full-Bridge inverter: f_{inv} = 8 kHz
DC-link voltage	V_{dc} = 450 V
Grid nominal voltage (RMS)	V_g = 230 V
Grid nominal frequency	ω_0 = 2π×50 rad/s

In the simulation, a 3-kW PV simulator has been adopted, where real-field solar irradiance and ambient temperature profiles are programmed. Fig. 17 shows the performance of the proposed high performance P&O-CPG method with two real-field daily conditions. In contrast to the conventional P&O-CPG method .the overshoots and power losses are significantly reduced by the proposed solution and a stable operation is also maintained. The algorithm also has a selective behavior to only react, when the fast irradiance condition is detected. This can be seen from the performance under clear irradiance conditions in Fig. 17(a), which is similar to the conventional P&O-CPG algorithm (shown in Fig. 17(a)).

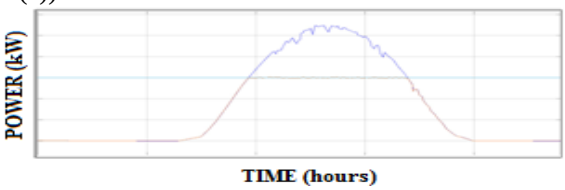

(a)

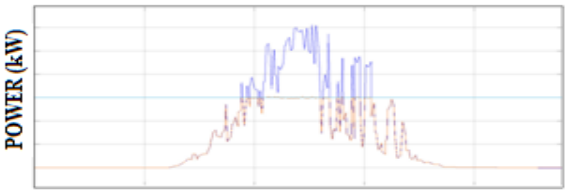

(b)

Fig. 17. simulation results of the proposed high-performance P&O-CPG algorithm under two daily conditions: (a) clear day and (b) cloudy day.

CONCLUSION

In this paper watched that a superior dynamic power control plot been constraining the greatest power which is nourish to the PV frameworks which is proposed there. The proposed arrangement ensure about the steady consistent power age operation. At the point when contrasted and the conventional techniques. Neuro fuzzy has many advantages i.e it can be stated that the normalized error obtained from neurofuzzy logic was lower. Here the proposed control methodology will powers the PV frameworks to work at the left half of the greatest power point, and which make to accomplish a steady operation alongside smooth changes. Neuro-fuzzy is a combination of ANN and fuzzy logic. By comparing all these techniques, the neuro-fuzzy controller is the lot of advantages, i.e the normalized error obtained from neuro fuzzy logic was lower. Reenactment have confirmed the viability of the proposed control arrangement with a specific end goal to limited power misfortunes, diminished overshoots and furthermore quick elements. In addition for single-arrange PV frameworks, same idea of CPG is likewise pertinent. In this way in such case, the PV voltage working extent will restricted and some little changes in the calculations which are important to ensure for a steady operation.

REFERENCES

[1] T. Stetz, F. Marten, and M. Braun, "Improved low voltage gridintegration of photovoltaic systems in Germany," IEEE Trans. Sustain. Energy, vol. 4, no. 2, pp. 534–542, Apr. 2013.

[2] A. Ahmed, L. Ran, S. Moon, and J.-H. Park, "A fast PV power tracking control algorithm with reduced power mode," IEEE Trans. Energy Conversion, vol. 28, no. 3, pp. 565–575, Sept. 2013.

[3] Y. Yang, H. Wang, F. Blaabjerg, and T. Kerekes, "A hybrid power control concept for PV inverters with reduced thermal loading," IEEE Trans. Power Electron., vol. 29, no. 12, pp. 6271–6275, Dec. 2014.
[4] German Federal Law: Renewable Energy Sources Act (Gesetz fur den Vorrang Erneuerbarer Energien) BGBl, Std., July 2014.
[5] Energinet.dk, "Technical regulation 3.2.5 for wind power plants with a power output greater than 11 kw," Tech. Rep., 2010.
[6] Y. Yang, F. Blaabjerg, and H. Wang, "Constant power generation of photovoltaic systems considering the distributed grid capacity," in Proc. of APEC, pp. 379–385, Mar. 2014.
[7] R. G. Wandhare and V. Agarwal, "Precise active and reactive power control of the PV-DGS integrated with weak grid to increase PV penetration," in Proc. of PVSC, pp. 3150–3155, Jun. 2014.
[8] W. Cao, Y. Ma, J. Wang, L. Yang, J. Wang, F. Wang, and L. M. Tolbert, "Two-stage PV inverter system emulator in converter based power grid emulation system," in Proc. of ECCE, pp. 4518–4525, Sept. 2013.
[9] A. Urtasun, P. Sanchis, and L. Marroyo, "Limiting the power generated by a photovoltaic system," in Proc. of SSD, pp. 1–6, Mar. 2013.
[10] S. B. Kjaer, J. K. Pedersen, and F. Blaabjerg, "A review of single-phase grid-connected inverters for photovoltaic modules," IEEE Trans. Ind. Appl., vol. 41, no. 5, pp. 1292–1306, Sept. 2005.

P. SUJATHA (PG Scholar)

Completed B.E in Electrical & Electronics Engineering in 2015 from DVR College Of Engineering & Technology JNTUH , HYDERABAD and Pursuing M.Tech form B. V Raju Institute Of Technology (Autonomous) College, Narsapur, Hyderabad, Telangana, India. Area of interest includes Electrical Power Systems.
E-mail id;sujatapothagoni@gmail.com

A. VIJAY KUMAR (Assistant Professor)

Completed B.Tech in Electrical &Electronics Engineering in 2005 From SSJ Engineering College, Affiliated JNTUH, Hyderabad and M.Tech in Control System in 2012 from ST. Mary's College Of Engineering And Technology Affiliated to JNTUH, Hyderabad. Working as Assistant Professor at B.V Raju Institute Of Technology (Autonomous) College, Narsapur, Hyderabad, Telangana, India. Area of interest includes Control Systems, Power Systems & MATLAB.
E-mail id: vijaykumar.a@bvrit.ac.in